Inverse identification of mechanical parameters of high-speed train suspensions submitted to random track irregularities

David Lebel, Christian Soize, Christine Funfschilling, Guillaume Perrin

Inverse identification of mechanical parameters of high-speed train suspensions submitted to random track irregularities

D. Lebel[a,b], C. Soize[a], C. Funfschilling[b] and G.Perrin[c]
[a]Multi-scale modeling and simulation (MSME UMR 8208 CNRS), Université Paris Est, France
[b]Innovation and Research department, SNCF, Paris, France
[c]CEA DAM DIF, Arpajon, France

Abstract: The objective of the work presented here is the inverse identification of parameters describing the mechanical characteristics of high-speed train suspensions for maintenance purposes. This identification is achieved by comparing simulation results to on-track accelerometric measurements. It requires the introduction of an output predictive error as a noise added to simulation outputs to take into account measure and model uncertainties, the introduction of an objective function defined on the parameter domain, and the optimization of this objective function, performed by an EGO (Efficient Global Optimization) algorithm thanks to the construction of a Kriging metamodel of the objective function.

1 Introduction

Trains dynamic behavior strongly relies on their suspensions state, which undergo damage throughout their lifetime. In order to ensure passengers safety and comfort, a good state of suspensions must be guaranteed, thanks to regular maintenance. Presently, this maintenance mostly relies on age or mileage criteria. The knowledge of the actual state of suspension characteristics could however allow the use of maintenance rules closer to the real needs. The industrial objective of the worked presented here is thus the development of a remote diagnosis method for high-speed train suspensions based on accelerometric on-track measurements. This work is part of a development project conducted by SNCF (the French National Railway Company).
Track geometry (also called track irregularities) constitutes the main excitation source of a rolling train, and has consequently a major influence on the train dynamic behavior (see [6, 10, 7, 8]). Track geometry is also subject to damage caused by railway traffic (see [9, 1]). In order to distinguish suspension damage from track geometry evolution in the accelerometric measurements in the train, railway dynamics simulation is necessary. More precisely, we propose to compare measured accelerations to simulated ones, computed on the track geometry which has been measured together with the accelerations. The experimental data (track geometry and accelerometric measurements) used for this work come from the train *IRIS 320*, a modified TGV specially equiped to perform various measurements at high speed (see [3, 2])
From a scientific point of view, this problem consists in a statistical inverse identification of the train model parameters describing the suspensions mechanical properties. The repetition of this identification on measurements performed at different times should allow for observing the time evolution of these parameters. Appropriate maintenance could then be triggered as soon as they leave the acceptable domain.

2 Description of the analyzed system

2.1 Mechanical system

In this work, the system considered is a train rolling at variable speed on a track characterized by its design and its geometry.
The track geometry is defined as the geometric irregularities of the rails position with respect to the theoretical track design. It can be modeled as a $\mathbb{R}^4$-valued stochastic process (see [11]). The track is divided in segments, a few kilometers each. For a fixed date, there is a given number of segments on which geometry has been measured. Consequently, a limited number of track geometry realizations is known, about one hundred. The input of the railway dynamical system is the excitation induced by the track geometry.
The train is described as a multibody model. It consists of rigid bodies linked together by mechanical joints (mostly stiffnesses and dampers) with nonlinear behavior. Wheel-rail contact law is also nonlinear. The train parameters involved in the identification process are solely mechanical parameters modeling the train suspensions. Certain suspension parameters will eventually be modeled as random variables, because their values are not known precisely. In this paper, we however present a first step for which they are taken deterministic. The railway dynamics software used for this work as a black box is *Vampire*.
The system output is the train accelerometric response to the track geometry at a certain (possibly varying) speed. For this work, only vertical and lateral accelerations on various points of the train carbodies and bogies are considered. The analysis of the response is done in the frequency domain.

2.2 Quantities of interest

Two different time scales are considered: the short-time scale associated with the train dynamics and the long-time scale associated with the evolution of the suspensions mechanical properties. For a fixed date (related to the long-time scale), the following quantities are defined:

- $\mathbf{X}(t)$ as a real vector-valued stochastic process indexed by the time interval $[0,T]$, representing the displacement condition imposed to each wheel of the train, in the axis system attached to the train, circulating at varying speed. Only a limited number of realizations of this stochastic process is known. These realizations are directly deduced from the geometry measurements, the train speed record and the location of the wheelsets along the train. In this work, no stochastic model of the track geometry is used.

- $\mathbf{A}(t)$ as a $\mathbb{R}^n$-valued stochastic process indexed by $[0,T]$, representing the train accelerometric response in the axis system attached to the train.

- $\mathbf{Y}(\omega)$ as a $\mathbb{R}^n$-valued stochastic process indexed by the frequency domain Ω, representing the amplitude of the Fourier transform of $\mathbf{A}(t)$ in dB:

$$\mathbf{Y}(\omega) = 10\log_{10}\left|\hat{\mathbf{A}}(\omega)\right|, \tag{1}$$

  with

$$\hat{\mathbf{A}}(\omega) = \int_0^T \frac{1}{\sqrt{T}}\mathbf{A}(t)e^{-i\omega t}dt\,. \tag{2}$$

- $\mathbf{w}$ as a deterministic vector with value in the admissible set $\mathcal{C}_{\mathbf{w}}$, subset of $\mathbb{R}^q$, representing the parameters describing the mechanical properties of the train suspensions.

The output quantity of interest is process $\mathbf{Y}$ rather than process $\mathbf{A}$. Only the amplitude of the Fourier transform is considered in order to avoid systematic phase-shift issues between measured and simulated processes in the time domain. This amplitude is taken in dB in order to characterize the system resonances as well as antiresonances.
The previous formulation is preferred to the computation of the power spectral density function of $\mathbf{A}$ because the emphasis is put on the calibration of the train model rather than on the analysis of the input variability propagation through the system. A similar approach could be performed with a fully deterministic track input. In that case the stochastic property of the output would only come from the uncertainty on the parameters, the computation of the power spectral density function would not be appropriate.
In the following sections, three different versions of process $\mathbf{Y}$ are used:

- $\mathbf{Y}^{\text{mes}}(\omega)$ directly computed from the accelerometric measurements.
- $\mathbf{Y}^{\text{sim}}(\omega, \mathbf{w})$ computed from the simulated accelerations, which depends on the $\mathbf{w}$ parameter.
- $\mathbf{Y}^{\text{mod}}(\omega, \mathbf{w})$ computed from $\mathbf{Y}^{\text{sim}}(\omega, \mathbf{w})$ to which a noise is added. This noise models the measurement and train model uncertainties (see Section 2.3).

2.3 Measure and train model uncertainties

To perform a correct parameter identification, it is necessary to introduce a model uncertainty to the simulation results $\mathbf{Y}^{\text{sim}}(\omega, \mathbf{w})$. An identification performed without uncertainty could result in nonrobust parameters, potentially very different from the real values. The simulation being used as a black box, the model uncertainty can only be introduced as an additive output predictive error. Moreover, a measurement uncertainty must be taken into account. These two types of uncertainty are globally introduced with an additive noise, $\mathbf{B}(\omega)$, on the response of the system. This noise must be identified from the available measurements. The noise identification is performed once and for all at a given reference date. It is then supposed than the identified process $\mathbf{B}(\omega)$ can be kept unchanged for all other dates. At reference date, accelerometric measurements provide a set of ν_0 sample paths $\{\mathbf{y}^{\text{mes},i}(\omega), \omega \in \Omega\}_{1 \leq i \leq \nu_0}$ of process $\{\mathbf{Y}^{\text{mes}}(\omega), \omega \in \Omega\}$. On the corresponding track irregularity measurements, a set of ν_0 sample paths $\{\mathbf{y}^{\text{sim},i}(\omega, \mathbf{w}_0), \omega \in \Omega\}_{1 \leq i \leq \nu_0}$ of process $\{\mathbf{Y}^{\text{sim}}(\omega, \mathbf{w}_0), \omega \in \Omega\}$ is computed by the simulation software. The nominal value of parameter $\mathbf{w}$ is denoted by $\mathbf{w}_0$. From those two sets, ν_0 sample paths of noise $\{\mathbf{B}(\omega), \omega \in \Omega\}$ are then computed:

$$\mathbf{b}^i(\omega) = \mathbf{y}^{\text{mes},i}(\omega) - \mathbf{y}^{\text{sim},i}(\omega, \mathbf{w}_0) \quad , \quad 1 \leq i \leq \nu_0 \,. \tag{3}$$

The stochastic process $\mathbf{B}$ is modeled as a Gaussian process independent from processes $\mathbf{Y}^{\text{mes}}$ and $\mathbf{Y}^{\text{sim}}(., \mathbf{w}_0)$. The mean and covariance functions of $\mathbf{B}$ are estimated by using the ν_0 sample paths $\{\mathbf{b}^i(\omega), \omega \in \Omega\}_{1 \leq i \leq \nu_0}$. Such a Gaussian model allows an easy sampling of process $\mathbf{B}$ to be generated.
Figure 1 shows the comparison between $\mathbf{Y}^{\text{mes}}(\omega)$ (black) with $\mathbf{Y}^{\text{sim}}(\omega, \mathbf{w}_0)$ (red) on the one hand (top graph), and $\mathbf{Y}^{\text{mes}}(\omega)$ (black) with $\mathbf{Y}^{\text{mod}}(\omega, \mathbf{w}_0)$ (blue) on the other hand (bottom graph), for the component k of these processes. This component corresponds to a carbody vertical acceleration. It can be noticed that the addition of the noise allows for obtaining a good match between the measured and the simulated mean functions. Moreover, the confidence region of process $\mathbf{Y}^{\text{mod}}$ overlaps the one of measured process $\mathbf{Y}^{\text{mes}}$.

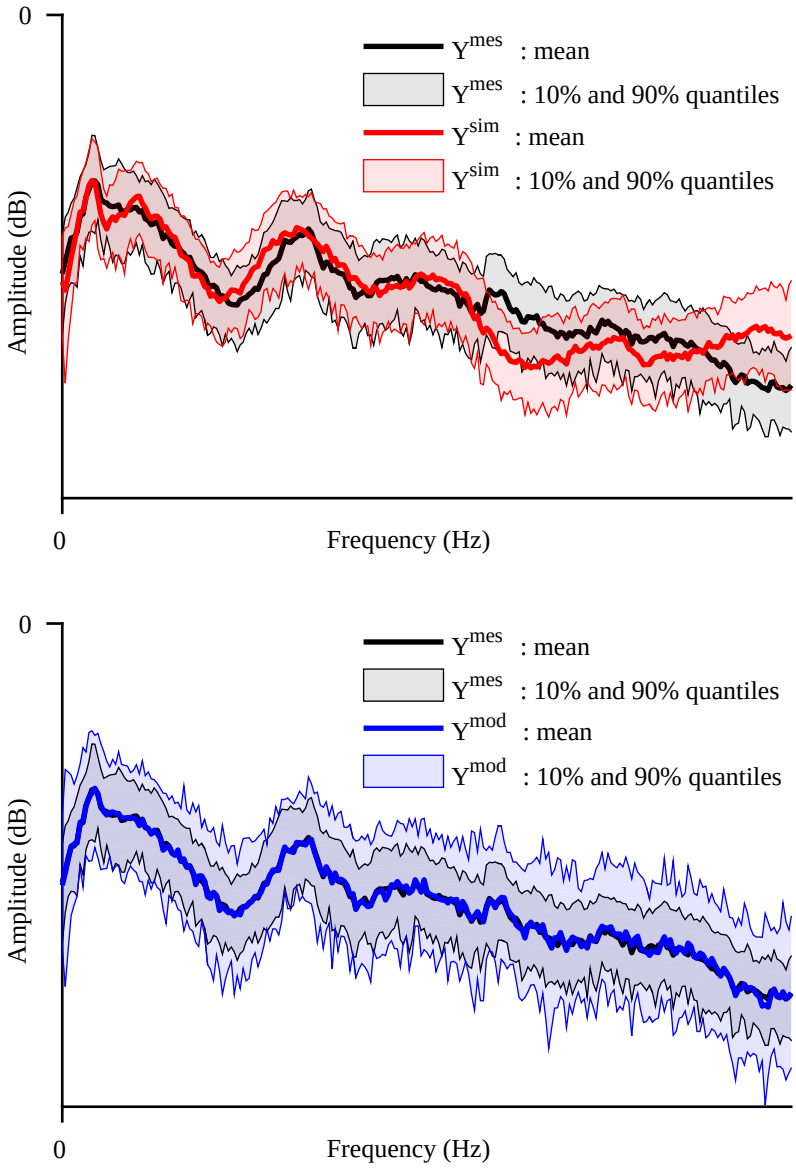

Figure 1: Mean and quantiles comparison of $Y_k^{mes}(\omega)$ with $Y_k^{sim}(\omega, \mathbf{w}_0)$ (top graph), and of $Y_k^{mes}(\omega)$ with $Y_k^{mod}(\omega, \mathbf{w}_0)$ (bottom graph), for the component k corresponding to a carbody vertical acceleration.

3 Estimation of the optimal model parameters with Kriging metamodel

This section presents an approach for the identification of an optimal deterministic parameter $\mathbf{w}_{\text{opt}}$, relying on Kriging metamodeling. For a given parameter $\mathbf{w}$, an objective function $\mathcal{J}(\mathbf{w})$ representing the distance between the measurements and the simulation results needs to be defined. A Kriging metamodel of this objective function is then built from an experimental design on $\mathcal{C}_{\mathbf{w}}$. The computation of $\mathbf{w}_{\text{opt}}$ is performed thanks to this metamodel. This procedure has been tested by using a numerical experiment.

For this part, all the quantities previously introduced are relative to the date at which the measurements have been made, which is different from the reference date used for the noise identification.

3.1 Definition of the objective function

In the present case, the objective function $\mathcal{J}$ is a real-valued function of the parameter $\mathbf{w}$ used to represent the distance between the processes $\mathbf{Y}^{\text{mes}}$ and $\mathbf{Y}^{\text{mod}}(.,\mathbf{w})$. The higher the objective function is, the smaller the distance between these processes will be. Consequently, in order to find the optimal parameter $\mathbf{w}_{\text{opt}}$ for which the simulation best matches the measurements, the objective function must be maximized:

$$\mathbf{w}_{\text{opt}} = \underset{\mathbf{w}\in\mathcal{C}_{\mathbf{w}}}{\arg\max}\left(\mathcal{J}(\mathbf{w})\right). \tag{4}$$

Two sets $\{\mathbf{y}^{\text{mes},i}\}_{1\leq i\leq \nu}$ and $\{\mathbf{y}^{\text{mod},i}(.,\mathbf{w})\}_{1\leq i\leq \nu}$ of ν sample paths of processes $\mathbf{Y}^{\text{mes}}$ and $\mathbf{Y}^{\text{mod}}(.,\mathbf{w})$ are known. For ω fixed in Ω, for $\mathbf{w}$ fixed in $\mathcal{C}_{\mathbf{w}}$, and for component k fixed in $\{1,\ldots,n\}$, the probability density functions of the real-valued random variables $Y_k^{\text{mes}}(\omega)$ and $Y_k^{\text{mod}}(\omega,\mathbf{w})$ are written as $p_{Y_k^{\text{mes}}}(.;\omega)$ and $p_{Y_k^{\text{mod}}}(.;\omega,\mathbf{w})$. They are estimated with the Gaussian kernel etimation method in the framework of nonparametric statistics from the realizations at each ω.
The objective function is defined according to equation (5):

$$\mathcal{J}(\mathbf{w}) = \sum_{k=1}^{n} \alpha_k \Psi_k(\mathbf{w}), \tag{5}$$

with $\sum_{k=1}^{n}\alpha_k = 1$. This equation aggregates the contribution of the different components of the $\mathbb{R}^n$-valued process $\mathbf{Y}$, with weights $\{\alpha_k\}_{1\leq k\leq n}$.
The function Ψ_k is constructed to compare the $\mathbb{R}$-valued processes Y_k^{mes} and $Y_k^{\text{mod}}(.,\mathbf{w})$. Two different constructions are proposed:

- The first one is inspired by the log-likelihood function (see [14]), written as:

$$\Psi_k(\mathbf{w}) = \frac{1}{|\Omega|}\int_{\Omega} \log \prod_{i=1}^{\nu} p_{Y_k^{\text{mod}}}(y_k^{\text{mes},i}(\omega);\omega,\mathbf{w}) d\omega. \tag{6}$$

- The second one is based on an overlaping criterion (see [4]), which computes the overlap between the probability density function $p_{Y_k^{\text{mes}}}(.;\omega)$ and $p_{Y_k^{\text{mod}}}(.;\omega,\mathbf{w})$:

$$\Psi_k(\mathbf{w}) = \frac{1}{|\Omega|}\int_{\Omega} \text{OVL}\left(p_{Y_k^{\text{mes}}}(.;\omega), p_{Y_k^{\text{mod}}}(.;\omega,\mathbf{w})\right) d\omega, \tag{7}$$

with

$$\text{OVL}(p_1,p_2) = 1 - \frac{1}{2}\int_{\mathbb{R}} |p_1(u) - p_2(u)|\, du. \tag{8}$$

3.2 Optimization with Kriging metamodel

In order to maximize a function $\mathcal{J}$ over the admissible set $\mathcal{C}_{\mathbf{w}}$, numerous calls to the function are necessary. In our case, the evaluation of objective function $\mathcal{J}$ requires the simulation of the train dynamic response over several hundreds of kilometers of track. The acceptable number of calls to the function is thus limited. This limitation becomes even more problematic as the dimension of the admissible set $\mathcal{C}_{\mathbf{w}}$ increases.
An optimization method with a limited number of calls to the function is proposed in [5]. This method, called the EGO algorithm (standing for Efficient Global Optimization) relies on the construction of a Kriging metamodel $\widetilde{\mathcal{J}}$ of the function $\mathcal{J}$ (see [12, 13]). It consists in a Gaussian stochastic process conditionned by the points where the value of the function $\mathcal{J}$ is known. The

construction of the metamodel requires a preliminary evaluation of $\mathcal{J}$ on a set $\{\mathbf{w}_j\}_{1\leq j\leq m_0}$ of m_0 points in $\mathcal{C}_\mathbf{w}$. This set is distributed as a space-filling experimental design on $\mathcal{C}_\mathbf{w}$, so that $\widetilde{\mathcal{J}}$ allows for approximating of $\mathcal{J}$ in the whole set $\mathcal{C}_\mathbf{w}$. Contrary to the use of the full computational model for evaluating the objective function, the use of the metamodel allows for quickly computing the objective function at any point in $\mathcal{C}_\mathbf{w}$. To find the optimum, the EGO algorithm then allows for computing at most m_1 new values of $\mathcal{J}$. The metamodel is used to determine the best location of these new points. The criterion used to designate the next candidate point is the expected improvement, defined on $\mathcal{C}_\mathbf{w}$ by the equation (9) (in the case when $\mathcal{J}$ needs to be maximized):

$$\mathrm{EI}(\mathbf{w}) = E\left\{\max(0, \widetilde{\mathcal{J}}(\mathbf{w}) - J_{\max})\right\}, \tag{9}$$

where $J_{\max}$ is the current known maximum of $\mathcal{J}$, and $E\{.\}$ denotes the mathematical expectation. The candidate point is the one that maximizes this expected improvement. The main interest of this criterion is that it offers a compromise between local search (where the metamodel mean function is maximum) and global search (where the objective function is poorly known). Objective function $\mathcal{J}$ is then evaluated on this candidate point. The current maximum $J_{\max}$ and the metamodel $\widetilde{\mathcal{J}}$ are then updated, and the search for a new candidate begins. If the maximum of expected improvement goes below a given tolerance ε, the search for new candidates is stopped, even though the acceptable number of new points m_1 is not reached. This stopping condition is set to avoid unnecessary iterations. This algorithm is summed up by the following pseudo code:

Initialize $\widetilde{\mathcal{J}}$ with the points $\{(\mathbf{w}_j, \mathcal{J}(\mathbf{w}_j))\}_{1\leq j\leq m_0}$
for $\ell = m_0+1 : m_0+m_1$ **do**
  Set $J_{\max} = \max_{j\in\{1,\ldots,\ell-1\}} \{\mathcal{J}(\mathbf{w}_j)\}$
  Set $\mathrm{EI} : \mathbf{w} \mapsto E\left\{\max(0, \widetilde{\mathcal{J}}(\mathbf{w}) - J_{\max})\right\}$
  Search $\mathbf{w}_\ell = \arg\max_{\mathbf{w}\in\mathcal{C}_\mathbf{w}} \{\mathrm{EI}(\mathbf{w})\}$
  if $\mathrm{EI}(\mathbf{w}_\ell) < \varepsilon$ **then**
    Break loop
  else
    Compute $\mathcal{J}(\mathbf{w}_\ell)$
    Update $\widetilde{\mathcal{J}}$ with the point $(\mathbf{w}_\ell, \mathcal{J}(\mathbf{w}_\ell))$
  end if
end for
Return $\mathbf{w}_{\mathrm{opt}} = \arg\max_{j\in\{1,\ldots,\ell-1\}} \{\mathcal{J}(\mathbf{w}_j)\}$

3.3 Optimization results on a numerical experiment case

The algorithm described in the previous section has been tested on a numerical experiment with the two types of objective function described in Section 3.1.

What we call here a numerical experiment is an artificial measurement generated by simulation with known suspension parameters. Let $\mathbf{w}_{\mathrm{ref}}$ be these known parameters representing damaged suspensions. The ν sample paths $\{\mathbf{y}^{\mathrm{sim},i}(.,\mathbf{w}_{\mathrm{ref}})\}_{1\leq i\leq\nu}$ of the dynamic response are computed by simulation with parameter $\mathbf{w}_{\mathrm{ref}}$. A set of ν sample paths $\{\mathbf{b}^i\}_{1\leq i\leq\nu}$ of the noise $\mathbf{B}$ are generated using the model identified in Section 2.3. This noise is added to the simulated response to obtain a reference response as close as possible from the measurements, but with known suspension parameters:

$$\mathbf{y}^{\mathrm{ref},i}(\omega) = \mathbf{y}^{\mathrm{sim},i}(\omega, \mathbf{w}_{\mathrm{ref}}) + \mathbf{b}^i(\omega) \quad , \quad 1 \leq i \leq \nu \,. \tag{10}$$

This set $\{\mathbf{y}^{\mathrm{ref},i}\}_{1\leq i\leq \nu}$ replaces set $\{\mathbf{y}^{\mathrm{mes},i}\}_{1\leq i\leq \nu}$ for the computation of the objective function.
For the test presented here, $\mathcal{C}_{\mathbf{w}}$ is a hypercube of dimension $q = 7$. The initial experimental design is a Latin Hypercube Sample of $m_0 = 500$ points, optimized with a maximin criterion. The tolerance ε for the stopping condition of the EGO algorithm is set at 10^{-4} times the size of the variation interval of the objective function. The two types of objective function have been tested, starting with the same initial experimental design. The weights $\{\alpha_k\}_{1\leq k\leq n}$ are chosen all equal to $\frac{1}{n}$.
Optimization results are presented in Table 1 and Figure 2. For each objective function, Table 1 gives the number of necessary iterations to reach stopping condition and the error between the reference and the estimated optimal value for each of the q components of parameter $\mathbf{w}$. This error is calculated as the difference between the reference and the estimated optimal value, in percentage of the length of the admissible interval of the corresponding component. Figure 2 represents the values of the different components of reference parameter $\mathbf{w}_{\mathrm{ref}}$ and estimated optimal parameter $\mathbf{w}_{\mathrm{opt}}$ on a normalized scale, that is to say, the admissible interval of each component has been shrinked to $[0\,,1]$.
The results of the optimization is globally satisfying. Apart from the second component that is discussed afterwards, the errors obtained with the overlap objective function are below 4% for every component. The likelihood objective function gives slightly better results on certain component, however its maximum error (on the third component) is bigger. Moreover, the optimization converges faster with the overlap objective function than with the likelihood one. If the second component can be ignored, the overlap objective function appears to be slightly better than the likelihood one.
The optimization result for the overlap function is bad on the second component. One can actually observe on Figure 2 that its value is stuck on the boundary of the admissible interval. This shows that this component could not be identified at all. An explanation for this is the fact that this second component is very coupled with the first one, while being significantly less influent on the measured acceleration. They both control stiffnesses linked to the vertical motion of the carbody, but the stiffness corresponding to the first component is located much closer to the sensor than the stiffness corresponding to the second component.

Table 1: Comparison of the optimization results using the two types of objective function: number of necessary iterations to reach stopping condition, and the error calculated as the difference between the reference and the optimal value in percentage of the admissible interval length, for each parameter component.

Objective function	Iterations	Error for each parameter component						
Likelihood	50	2.4	5.2	7.4	2.4	1.8	0.4	3.2
Overlap	18	2.9	25	3.6	0.04	1.1	1.1	3.9

4 Conclusion and perspectives

In this paper, we have presented a robust identification method by solving a statistical inverse problem. This method allows for identifying the mechanical parameters of high-speed train suspensions, through the use of on-track measurements and railway dynamic simulation. This method focuses on the optimization of an objective function with the EGO algorithm using a Kriging metamodel of this objective function. This optimization has been tested on a numerical experiment. Results are promising for the two types of objective function that have been

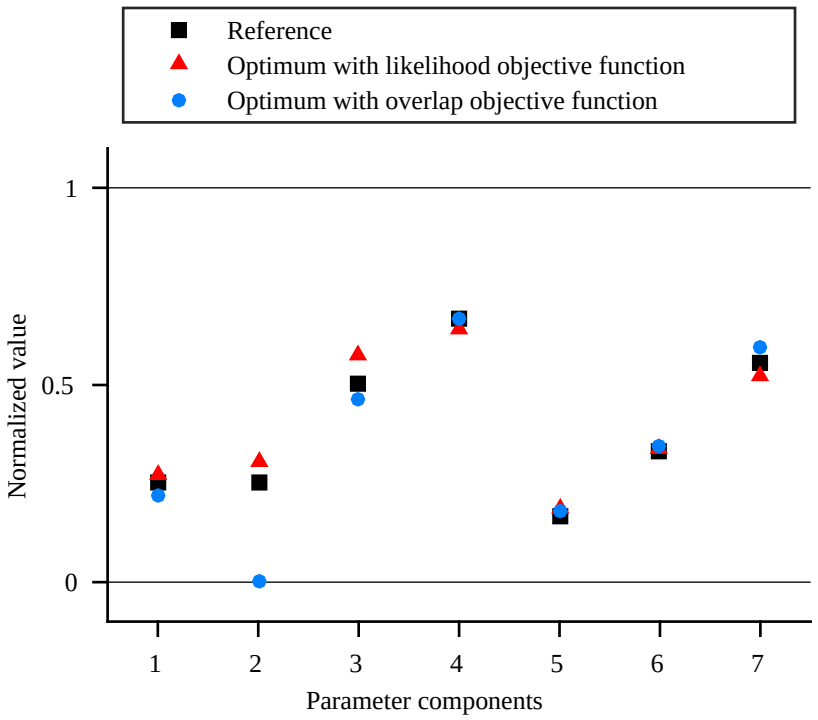

Figure 2: Optimization results: $\mathbf{w}^{opt}$ for likelihood objective function (red triangles) and overlap objective function (blue dots) are compared component by component to $\mathbf{w}^{ref}$ (black squares) on a normalized scale.

proposed. The validation on actual measurements is in progress.
For this work, the mechanical parameters have been kept deterministic. The results obtained here set a good basis for the introduction of uncertainties on the parameters. The identification would then concern the probability distribution of these parameters.

Acknowledgement

This research has been supported by *SNCF*, the French National Railway Company.

References

[1] A. J. Bing and A. Gross. “Development of railroad track degradation models”. In: *Transportation research record.* 939 (1983), pp. 27–31.

[2] F. Coudert and B. Richard. “IRIS 320 GEOV: un nouveau système de mesure de la géométrie de la voie, réalisé dans la continuité des voitures Mauzin”. In: *Revue générale des chemins de fer* Jun (2009), pp. 7–22.

[3] G. Foeillet, F. Coudert, and V. Delcourt. “IRIS 320 is a global concept inspection vehicle merging engineering and R&D tools for infrastructure maintenance”. In: *Proceedings of the Eight World Congress on Railway Research*. Seoul, South Korea, 2008.

[4] H. F. Inman and E. L. Bradley. “The overlapping coefficient as a measure of agreement between probability distributions and point estimation of the overlap of two normal densities”. In: *Communications in Statistics - Theory and Methods* 18.10 (1989), pp. 3851–3874.

[5] D. R. Jones, M. Schonlau, and W. J. Welch. “Efficient Global Optimization of Expensive Black-Box Functions”. In: *Journal of Global Optimization* 13 (1998), pp. 455–492.

[6] T. Karis. “Track Irregularities for High-Speed Trains”. Master thesis. KTH University, 2009.

[7] N Lestoille, C Soize, and C Funfschilling. “Sensitivity of train stochastic dynamics to long-time evolution of track irregularities”. In: *Vehicle System Dynamics* 54.5 (2016), pp. 545–567.

[8] N. Lestoille, C. Soize, and C. Funfschilling. “Stochastic prediction of high-speed train dynamics to long-term evolution of track irregularities”. In: *Mechanics Research Communications* 75 (2016), pp. 29–39.

[9] A. López-Pita et al. “Maintenance Costs of High-Speed Lines in Europe: State of the Art”. In: *Transportation Research Record: Journal of the Transportation Research Board* 2043 (2008), pp. 13–19.

[10] G. Perrin et al. “Quantification of the influence of the track geometry variability on the train dynamics”. In: *Mechanical Systems and Signal Processing* 60 (2015), pp. 945–957.

[11] G. Perrin et al. “Track irregularities stochastic modeling”. In: *Probabilistic Engineering Mechanics* 34 (2013), pp. 123–130.

[12] J Sacks et al. “Design and Experiments of Computer Experiments”. In: *Statistical Science* 4.4 (1989), pp. 409–423.

[13] T. Santner, B. Williams, and W. Notz. *The Design and Analysis of Computer Experiments*. New York: Springer-Verlag, Berlin, 2003, p. 283.

[14] J. C. Spall. *Introduction to Stochastic Search and Optimization : Estimation, Simulation and Control*. John Wiley & Sons, 2003, p. 618.